Support for the value 5/2 for the spin glass lower critical dimension at zero magnetic field

Andrea Maiorano[a,b,1,2] **and Giorgio Parisi**[a,c,1,2]

[a]Dipartimento di Fisica, Sapienza Università di Roma, 00185 Rome, Italy; [b]Instituto de Biocomputación y Física de Sistemas Complejos (BIFI), 50018 Zaragoza, Spain; and [c]Istituto Nazionale di Fisica Nucleare, Sezione di Roma I, Insitute of Nanotechnology (Nanotec), Consiglio Nazionale delle Ricerche (CNR), 00185 Rome, Italy

Contributed by Giorgio Parisi, April 9, 2018 (sent for review December 1, 2017; reviewed by Stefan Boettcher and Alexander Karl Hartmann)

We study numerically various properties of the free energy barriers in the Edwards–Anderson model of spin glasses in the low-temperature region in both three and four spatial dimensions. In particular, we investigated the dependence of height of free energy barriers on system size and on the distance between the initial and final states (i.e., the overlap distance). A related quantity is the distribution of large local fluctuations of the overlap in large 3D samples at equilibrium. Our results for both quantities (barriers and large deviations) are in agreement with the prediction obtained in the framework of mean-field theory. In addition, our result supports $D_{lc} = 2.5$ as the lower critical dimension of the model.

spin glasses | barriers | correlations

Many materials undergo a phase transition at sufficiently low temperatures. It is believed that these phase transitions may be grouped into universality classes: Each universality class displays its unique behavior and in the case of second-order phase transitions, each class has its own critical exponents. Inside each universality class, the study of the phase transitions at space dimensions different from three is a source of inspiration for understanding how a system behaves in our 3D world. Especially in the case of second-order phase transitions it very important to get a qualitative understanding of the properties of the system in the temperature–dimensions plane.

Let us consider a second-order transition characterized by a disordered high-temperature phase and with an ordered low-temperature phase. Usually, there are two special values of the space dimensions D:

i) The upper critical dimension (D_{uc}): The critical exponents are given by the mean-field ones for space dimensions D higher than the upper critical dimension; they are nontrivial functions of the dimension D below D_{uc}.

ii) The lower critical dimension (D_{lc}): The low-temperature phase disappears for dimensions less than D_{lc}. In many cases, the transition temperature becomes zero when we approach D_{lc} and it is exactly zero at $D = D_{lc}$.

The lower and upper critical dimensions are universal quantities (as well as the critical exponents), in the sense that they do not depend on the microscopic details of the Hamiltonian of the system. We can check the soundness of our command of the physics of a model by trying to compute these two dimensions. Failure in doing that is a symptom that we have missed some crucial understanding. Indeed, ignoring the upper and/or the lower critical dimensions is actually a serious lack of understanding: In particular, ignoring the lower critical dimensions means we lack a good description of the mechanisms that lead to the disappearance of the low-temperature ordered phase at low dimensions.

The success of the perturbative renormalization group techniques applied to the ferromagnetic phase transition in 3 dimensions (1–3) is bound to the quantitative determination of the upper critical dimension ($D_{uc} = 4$ in this case), which in turn allowed for the quantitative control of the infrared stable fixed point and anomalous dimensions of operators in $4 - \epsilon$ dimensions and led to the ϵ expansion for the critical exponents. A similar approach is suitable for obtaining useful information starting from the knowledge of the lower critical dimension: For example, in the case of spontaneous breaking of a continuous conventional symmetry [e.g., $O(N)$, $D_{lc} = 2$] one can derive a $2 + \epsilon$ expansion (4–7).

In the case of glassy systems, one of the theoretical difficulties is a lack of precise knowledge about the lower critical dimension: In the case of structural glasses, there is still a debate about whether a glass transition is present in three dimensions. The best-studied case is Ising spin glasses at zero magnetic field (i.e., the Edwards–Anderson model). The presence of a low-temperature phase in three dimensions has been proved experimentally and very large-scale numerical simulations do confirm the experimental result. Franz, Parisi, and Virasoro (8) (FPV) many years ago performed an analytic computation of the interface free energy between different low-energy phases. (An explicit computation shows that both the internal energy and the entropy increase have a similar behavior to the one of the free energy.) A byproduct of this computation is the prediction that the lower critical dimension for spin glasses at zero magnetic field is $5/2$. This paper aims to verify numerically the correctness of the FPV formulas for the energy and the free energy of interfaces between different phases, adding additional evidence that the lower critical dimension is $5/2$ in the case of Ising spin glasses at zero magnetic field. Before presenting our numerical results, we recall the relationship between the interface free energy cost

Significance

Glassy systems at low temperature may stay in many equilibrium configurations quite different from one another. An important quantity is the (free) energy difference for going from an equilibrium configuration to another one: Its properties dominate the dynamics at large times. The analytic computation of these differences is notoriously difficult. For spin glasses a clean computation can be done, using uncontrolled approximations. Here we use numerical simulations to show that this theory predicts the correct properties of the differences in three and four dimensions. The same theory predicts also that the spin glass transition disappears at dimensions 5/2 and our verification of the predictions of the theory brings support to this result.

Author contributions: A.M. and G.P. designed research, performed research, contributed new reagents/analytic tools, analyzed data, and wrote the paper.

Reviewers: S.B., Emory University; A.K.H., Oldenburg University.

The authors declare no conflict of interest.

[1]A.M. and G.P. contributed equally to this work.

[2]To whom correspondence may be addressed. Email: giorgio.parisi@roma1.infn.it or andrea.maiorano@roma1.infn.it.

This article contains supporting information online at www.pnas.org/lookup/suppl/doi:10.1073/pnas.1720832115/-/DCSupplemental.

Published online May 1, 2018.

and the lower critical dimension and recapitulate some known properties of spin glasses.

In the case of the Ising ferromagnet ($D_{lc}=1$) and for a Heisenberg isotropic ferromagnet ($D_{lc}=2$), the value of the lower critical dimensions can be computed by a simple qualitative argument based on the cost of the free energy for creating an interface between two regions with different values of the order parameter. There is general consensus on the impossibility of long-range order when such cost is finite in the thermodynamic limit. Sometimes the computation can be simplified by computing the increase in the ground-state energy at zero temperature upon changing the boundary conditions in an appropriate way.

Let us see how to do such a computation in the Ising ferromagnet: The spins are ± 1 variables. We consider a D-dimensional system, with periodic conditions in all directions $x_2, \ldots, x_D$, but in the $x_1 \equiv x$ direction where we impose fixed boundary conditions. In the plane $x=0$ we set $\sigma=1$ and in the plane $x=L-1$ we set either $\sigma=1$ (periodic boundary conditions) or $\sigma=-1$ (antiperiodic boundary conditions). Our aim is to compute the ground-state energy difference as a function of L. In the case of periodic boundary conditions the ground state is all σs equal to 1, while in the case of antiperiodic boundary conditions the ground state is given by $\sigma(\vec{x})=1$ for $x_i < M$, $0<M<L-1$ and $\sigma(\vec{x})=-1$ for $x_i \geq M$. We immediately get that the variation $\Delta E(L)$ of the energy is $2L^{D-1}$.

If we are interested in computing the free energy difference at nonzero temperature, not too near the critical point, we can write a Landau–Ginzburg-like expression for the magnetization $m(\vec{x})$. We find that the variation of the free energy is $\Sigma(T)L^{D-1}$, where $\Sigma(T)$ is the surface tension. The free energy increase of the free energy in $D=1$ goes to a constant for large L and therefore $D_{lc}=1$ is the lower critical dimension.

In the planar spin model case spin waves are present and we can have smooth interfaces with much lower free energy cost. In this model the spins are 2D vectors of modulus 1 and they can be parameterized as $\sigma(\vec{x})=\{\cos(\theta(\vec{x})), \sin(\theta(\vec{x}))\}$. Neglecting vortices, in the continuum limit the phase $\theta(\vec{x})$ is a smooth function. In the low-temperature regime we can write an effective free energy as

$$AL^{D-1}\int d^D x \left(\frac{d\theta(\vec{x})}{dx}\right)^2, \qquad [1]$$

where $\theta(\vec{x})$ denotes the direction of the magnetization around the point $\vec{x}$ and A is a positive constant. This expression can be derived from a Landau–Ginsburg functional (or equivalently from the Goldstone model) where one neglects the longitudinal fluctuations in the direction of the magnetizations.

In this case we can introduce more complex boundary conditions: e.g., $\theta(x_1)|_{x_1=0}=0$ and $\theta(x_1)|_{x_1=L-1}=\theta_B$. A detailed computation (*SI Appendix, Barriers in the Heisenberg Ferromagnet*) tells us in this case we can construct an interface where the phase $\theta(\vec{x})$ is a smooth function. We find that the free energy increases as $AL^{D-2}\theta_B^2$, and hence $D_{lc}=2$. A similar result is obtained for the internal energy. Indeed in $D=2$ these differences remain of order 1 and also when $L\to\infty$.

The absence of a phase with a nonzero order parameter in 2D systems is the essence of the Mermin–Wagner–Hohenberg (9, 10) theorem where one studies small fluctuations around equilibrium, proving that in the presence of the nonzero order parameter the correlation function in the small-momentum region behaves as $1/k^2$ (i.e., a Goldstone Boson is present) and this behavior is inconsistent in a 2D world.

A popular model of spin glasses at zero magnetic field is the Edwards–Anderson (EA) model (11) in which the Ising spins $\{\sigma\}$ are arranged on a D-dimensional cubic lattice. Only interactions among nearest-neighbors pairs contribute to the energy: The Hamiltonian is given by

$$H=-\sum_{\langle i,k\rangle} J_{i,k}\sigma_i,\sigma_k, \qquad [2]$$

where the $J_{i,k}=\pm 1$ are quenched (frozen) random couplings. Different realizations of the configuration of couplings $\{J\}$ define different instances (or samples) of the system. Two or more independent copies of the same instance are called replicas.

In the low-temperature phase a crucial quantity that plays the role of order parameter is the expectation value of the overlap $q_i \equiv \sigma_i\tau_i$, where σ_i and τ_i are spins at site i in any two independent equilibrium configurations. We define the intensive value of the overlap in a box of linear size L as

$$Q=\frac{1}{L^D}\sum_i q_i. \qquad [3]$$

In the mean-field approximation the thermal average $\langle Q^2\rangle_J$ for a given disorder instance is nonzero below the transition temperature in the infinite-volume limit. For a given sample the overlap may take many different values and with changes in the extensive free energy that are of order 1: In other words there are globally different arrangements of the spins that have comparable probabilities. As a consequence the overlap probability distribution function $P_J(Q)$ (details in *SI Appendix, The Definition of the Order Parameter in Mean Field Theory*) is of order 1 for many different values of Q: $P_J(Q)$ depends on the choice of the Js (nonself averageness); also $\langle Q^2\rangle_J$ depends on the values of the Js. If we take two different equilibrium configurations of the system (e.g., $\{\sigma\}$ and $\{\tau\}$), their global overlap Q can be in the range $[-q_{EA} : q_{EA}]$, where, denoting by $[\cdots]_J$ the average over samples, $q_{EA}=\left[\langle s_i\rangle^2\right]_J$ is the so-called EA order parameter, without any additional cost. The Q-constrained free energy density $F(Q)$ is constant in this interval as shown by an explicit computation. The existence of flat regions in free energy has deep consequences.

The mean-field theory is relatively well understood: It is valid in the simple Sherrington–Kirkpatrick model that naively corresponds to the infinite-dimensional limit of the EA model. In finite dimensions, the analytic studies are more complex. Standard arguments can be used to construct a low-momentum effective Landau–Ginzburg theory and apply renormalization group-like techniques (12, 13). The system has a standard second-order phase transition with a divergent nonlinear susceptibility $\chi^{(3)}(T)\propto(T-T_c)^{-\gamma}$. It has been shown that in dimensions greater than 6 the critical exponents are those of mean field (i.e., $\gamma=1$). An ϵ expansion for the critical exponents has been constructed in $\epsilon=6-D$ (14): The series were computed up to the order ϵ^3 (15) but unfortunately the convergence of the series is not good and it is difficult to use them already in dimensions $D=5$.

Quite accurate experiments (16) and numerical simulations (17, 18) agree on the existence of a transition in dimensions $D=3$, with quite a large value of γ (i.e., $\gamma\approx 6$), and therefore $D_{lc}<3$. On the contrary in dimensions $D=2$ the nonlinear susceptibility is finite at any positive temperature and it has a power-law divergence in the zero-temperature limit. According to standard folklore, at the lower critical dimensions, the relevant susceptibility should diverge exponentially when the temperature goes to zero and a power-law divergence should be present only below the lower critical dimensions. Numerical simulations done by Boettcher (19, 20) give $D_{lc}=2.4986$ with a small error. Boettcher studies the exponent that controls the dependence on L of the variance of the energy difference from periodic to antiperiodic boundary conditions for different dimensions D. This exponent should change sign at the lower critical dimension: Its value is obtained by interpolating (as a function

of the dimensions D) this critical exponent. A similar estimate $D_{lc} = 2.491$ (not as accurate as the previous one) comes from the extrapolation of the values of the critical temperature (21) as a function of dimensions, assuming that T_c vanishes proportionally to $\sqrt{D - D_{lc}}$, as suggested by theoretical considerations (22).*

Summarizing, numerical simulations and experiments tell us that $2 < D_{lc} < 3$. There are also strong numerical pieces of evidence that the value of D_{lc} is quite near to and likely equals $5/2$. [We expect that the upper and the lower critical dimensions are simple rational numbers in the rare case that they are not integers (noninteger values are possible: For example, the upper critical dimension for a quadricritical point—that is represented by a ϕ^8 interaction—is $8/3$).]

The value $D_{lc} = 5/2$ was predicted in 1993, way before Boettcher's work, in a remarkable paper (8) assuming that there are minimal corrections to mean-field theory predictions. (It was assumed that we have a Landau–Ginsburg-type functional whose form is obtained by neglecting loop corrections to mean-field theory.)

We have seen that we can define a free energy as a function of the global overlap Q and the Q-constrained free energy density $F(Q)$ is constant for $|Q| < q_{EA}$. A natural question arises when we constrain two different large regions of the system to have two different values of Q. The bulk contribution to the free energy vanishes, and the contribution coming from the interface that we have to evaluate remains.

In ref. 8, FPV considered two systems A and B with the same Hamiltonian (i.e., same $\{J\}$) inside a D-dimensional box of side L. Using the same geometry that we discussed above, they studied the free energy increase when we constrain the two systems to have a mutual overlap Q^{AB} with a value $Q^{AB} = Q$ on a plane on the boundary at $x = 0$ and $Q^{AB} = Q' = Q + \Delta$ at the other boundary at $x = L$. The computation was done for small Δ in the region where both Q and Q' are in the range $[-q_{EA} : q_{EA}]$. We can write $q(x) = Q + \theta(x)$ with

$$\theta(0) = 0 \quad \text{and} \quad \theta(L) = \Delta. \qquad [4]$$

We can thus compute the free energy cost by using a variational procedure with respect to all other variables (i.e., probability distribution of all of the overlaps Q^{AA} for system A and Q^{BB} for system B and all of the overlaps Q^{AB} except those on the boundary). We finally arrive at the expression for the free energy increase $\Delta F_L[\theta]$ that is a functional of $\theta(x)$. At the end of the day, we have to minimize $\Delta F_L[\theta]$.

The results of this explicit computation were rather surprising. A simple quadratic analysis of the free energy (we keep the quadratic terms in θ in the free energy or equivalently the linear ones in the mean-field equations) implies that the final result is the sum of a few terms of the form

$$\Delta F_L[\theta] = A L^{D-1} \int_0^L dx \left(\frac{d\theta(x)}{dx} \right)^2. \qquad [5]$$

However, when all of the terms are assembled, these quadratic contributions cancel out. No free energy increase is present if we consider only quadratic terms.

If we keep higher-order terms (e.g., the cubic terms), we get nonlinear terms in the mean-field equations. Finally we obtain the amazing result:

$$\Delta F_L[\theta] \propto L^{D-1} \int_0^L dx \left(\frac{d\theta(x)}{dx} \right)^{5/2}. \qquad [6]$$

This result can also be generalized to the case of a function $\theta(\vec{x})$ that depends on all of the coordinates of $\vec{x}$:

$$\Delta F_L[\theta] \propto \int_0^L dx^D \left(\sum_{\nu=1,D} \left(\frac{\partial \theta(\vec{x})}{\partial x_\nu} \right)^2 \right)^{5/4}. \qquad [7]$$

We finally obtain that the free energy increase is given by

$$\Delta F(L, \Delta) \equiv \min_\theta \Delta F_L[\theta] \propto L^{D-5/2} \Delta^{5/2}, \qquad [8]$$

where the minimum is done over all of the functions $\theta(x)$ that satisfy the boundary conditions, Eq. **4**. A similar expression is obtained for the internal energy.

This analysis implies that the barriers are much smaller than in the known cases of spontaneous breaking of a continuous symmetry (the nature of the Goldstone modes is quite different). At the end we find that the barriers vanish for $D \leq 2.5$, and hence $D_{lc} = 2.5$.

Results and Discussion

It is clear that the validity of the FPV result, which has been derived in the mean-field framework, can be considered doubtful. However, a similar result also holds in the ferromagnetic case, when other properties of mean-field theory are not valid. Indeed, detailed arguments show that the interaction of Goldstone Bosons (magnons in this case) is essentially the same as in mean-field theory.

The FPV theory predicts a value of the lower critical dimension that is very near the one suggested by earlier numerical simulations. To check its validity beyond the assumptions used for its derivation, we investigated the agreement of its predictions with the results of purposely designed numerical simulations. As we shall see the results are in remarkable agreement.

We consider two different kinds of simulations: the direct measurement of the interface energy and the study of large deviations of the overlap differences in the same sample at equilibrium.

Direct Measurement of the Interface Energy. We computed directly the interface energy $\Delta E(L, Q, \Delta)$ in $D = 3$ and $D = 4$ in the most extreme case $Q = 0$ and $\Delta = 2$; i.e., $Q = 1$ on one boundary and $Q = -1$ on the other boundary. We studied this extreme case for two reasons: The signal-to-noise ratio is higher and its numerical implementation is much simpler than that in the case where $\Delta < 2$.

An FPV computation predicts that both the interface energy $\Delta E(L)$ and interface free energy $\Delta F(L)$ grow as $L^{1/2}$ for $D = 3$ and as $L^{3/2}$ for $D = 4$. We studied only the internal energy that can be computed in a much simpler way than the free energy.

The data we discuss below were produced by simulations of the EA model Eq. **2** with binary couplings ($J_{ij} = \pm 1$ with equal probability) in $D = 3$ and $D = 4$. (see Methods for details). The critical temperature for the model is $T_c \simeq 1.103$ in $D = 3$ (23) and $T \simeq 2.0$ in $D = 4$ (24–26). We performed our simulations at a temperature of the order of $0.7\,T_c$. At this value of the temperature thermalization of the samples is not too difficult, and we are far enough from the critical temperature for simulations to be not too sensitive to crossover effects. More precisely our simulations were done at $T = 0.7 \simeq 0.64\,T_c$ in $D = 3$ and at $T = 1.4 \simeq 0.7\,T_c$ in $D = 4$.

We report data for the square of the interface energy $\Delta E(L)^2$ as a function of the linear size up to L for both $D = 3$ (up to $L = 20$) and $D = 4$ (up to $L = 12$) in Fig. 1.

A linear growth of $\Delta E(L)^2$ describes very well the $D = 3$ data, in very good agreement with the theoretical prediction that gives

*A less quantitative prediction comes from the value of the exponent η as a function of the dimensions D. This exponent strongly decreases when going from dimensions 4 to dimensions 3 where its value is $\eta(3) = -0.39 \pm 0.1$ (23). We expect that at the critical dimensions $D_{lc} = 2 - \eta(D_{lc})$ a simple extrapolation of $\eta(D)$ would give $D_{lc} \approx 2.6$ with large errors. If we assume that $\eta(D)$ is a decreasing function of D (as happens in all the extrapolations), the 3D value implies that $D_{lc} > 2.4$.

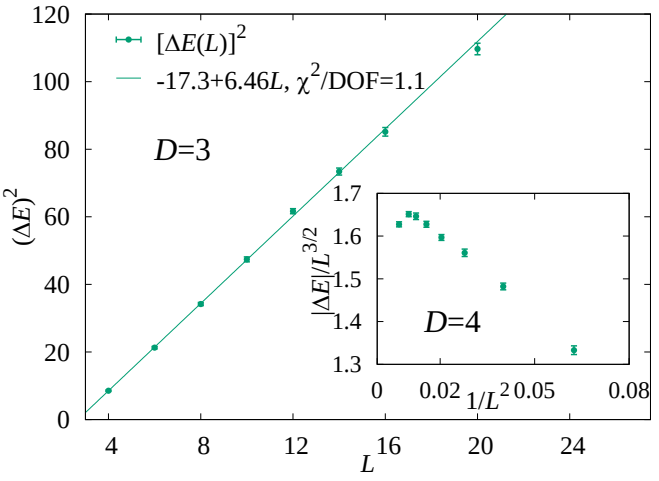

Fig. 1. Main plot, $D=3$: $\Delta E(L)^2$ as a function of L at $T=0.7$. The theory predicts an asymptotic linear behavior. In *Inset*, $D=4$: $\Delta E(L)/L^{3/2}$ as a function of $1/L^2$ at $T=1.4$. The theory predicts a finite nonzero limit at $1/L=0$.

$\Delta E(L) \propto L^{1/2}$. A linear fit to $\Delta E(L)$ works surprisingly well also at L as small as 4 up to the largest value of L, i.e., $L=20$. The reasons for such small finite-size corrections in $D=3$ are unclear.

In dimensions $D=4$ data have stronger finite-size corrections, but the ratio $|\Delta E(L)|/L^{3/2}$ tends to saturate at larger sizes. Unfortunately, we are limited to considering values of L up to 12 in $D=4$ that correspond to 20,736 spins, a number already much larger than the number of spins (8,000) that we used in $L=20$ for $D=3$.

Both 3D and 4D data strongly support the prediction $\Delta E(L) \propto L^{D-5/2}$.

The results we obtain for the scaling exponent of energy differences are larger than previous numerical estimates by measuring the energy cost of flipping boundary conditions in ground-state computations (21, 27, 28). We stress we have a completely different setting here, the main difference being the imposed constraint (fixed total overlap Q and overlap difference between opposite boundaries Δ) determining completely different excitations (discussion in *SI Appendix, Comparison to Previous Estimates of the Stiffness Exponent*).

Large Deviations of Local Overlap Fluctuations in a Sample. We could use the previous approach to study also the Δ dependence of the energy barriers by performing a different simulation for each value of Δ. Here we prefer to do the direct tests of Eq. **8** for the free energy, computing the probability of rare configurations in existing large-scale simulations performed by the Janus Collaboration (29–31).

In the low-temperature phase, the local overlaps $q(\vec{x})$ of two equilibrium configurations should fluctuate around the volume average of q, i.e., Q. The probability of having a rare fluctuation with an overlap value q significantly different from Q in a large region is exponentially damped and it can be computed starting from Eq. **6**. The computation could be done by means of a standard simulation of spin glasses and looking for the probability distribution of these rare events. A computation along this baseline for hierarchical spin glass models on Dyson lattices can be found in ref. 32. We find it convenient to use the large database of the Janus Collaboration that contains already thermalized spin glass configurations for quite large lattices (up to $L=32$ and down to $T=0.64T_c$ in $D=3$).

The region where we look for large fluctuations of Q may be a cube, as in the case of window overlaps; however, in this case we consider a very simple geometric setting. Let us define the quantities of interest. We work in $D=3$ in a box of size L with periodic boundary conditions. We define the overlap $q_{M,x}$, obtained by averaging the local overlap in a region of size $L^2 \times M$ delimited by $x \le i_x \le x+M-1$:

$$q_{M,x} = \frac{1}{ML^2} \sum_{x \le i_x \le x+M-1} \sum_{i_y, i_z} q(i_x, i_y, i_z). \qquad [9]$$

We are interested in computing the probability of having $q_{M,x}$ quite different from the global average Q. To simplify the analysis we define $\Delta_M = \frac{1}{2}|q_{M,x} - q_{M,x+L/2}|$, i.e., the difference in the overlap of two regions of size $L^2 \times M$ that are at the largest possible distance (we are using periodic boundary conditions), normalized in $[0,1]$.

The quantity of interest is the probability density of Δ_M inside a box of size L, i.e., $P_M(\Delta_M, L)$, with fixed total overlap in the two regions $Q_M = |q_{M,x} + q_{M,x+L/2}|$, in the large-deviation region where this probability is small; we consider $Q_M = 0$ (*Methods*), allowing for the largest range of fluctuations Δ and more statistics in the large-deviation region. We average $P_M(\Delta_M, L)$ over all samples. In the large-deviation region, this probability is given by the exponential of the free energy difference multiplied by $-\beta$. The prediction of FPV is

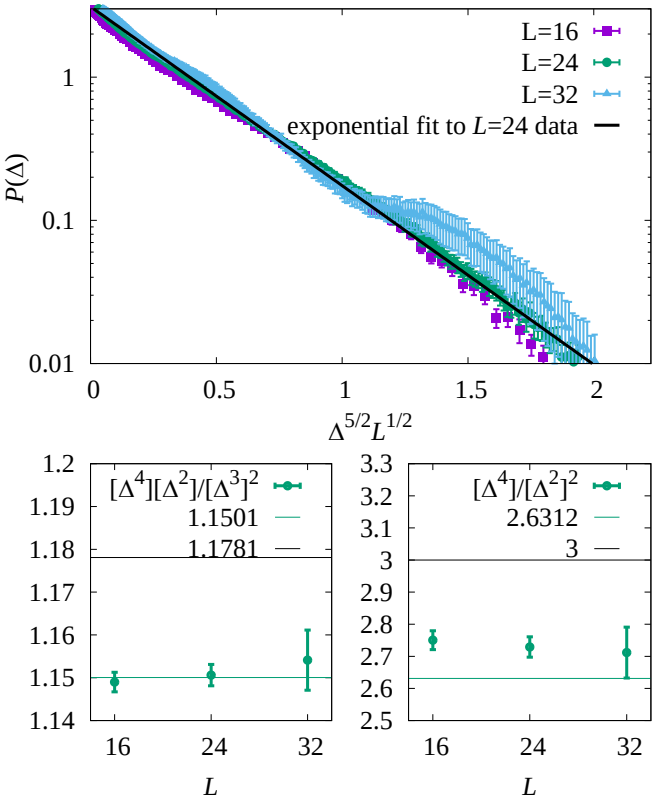

Fig. 2. (*Top*) $P(\Delta_M, L)$, $M/L=1/8$ (*Large Deviations of Local Overlap Fluctuations in a Sample*) as a function of $z \equiv L^{1/2}\Delta^{5/2}$, $T \simeq 0.64T_c$. (*Bottom*) Comparison of cumulants obtained from the numerical data (points with error bars) and values obtained with the prediction Eq. **10** (green line) and expected for a Gaussian distribution (black line). (*Bottom Right*) The kurtosis K. (*Bottom Left*) The cumulant ratio R (see *Large Deviations of Local Overlap Fluctuations in a Sample*).

$$P_M(\Delta_M, L) \propto \exp\left(-A_{M,L} L^{1/2} \Delta_M^{5/2}\right) \qquad [10]$$

in the large-deviation region $z \equiv L^{1/2}\Delta_M^{5/2} >> 1$ and Δ_M not too large. The coefficient $A_{M,L}$ does depend on the details of the free energy and therefore it cannot be computed; however, we can compute its dependence on M: As we shall see it turns out to be a function of M/L.

We plot $P_M(\Delta_M, L)$ in $D=3$ at $T=0.7$ as a function of $z = L^{1/2}\Delta^{5/2}$ for $L=16, 24, 32$ and $M/L=1/8$ in Fig. 2, *Top*. The $L=32$ data at the largest z values are noisy, due to the lower statics that we have at this value of L. The theoretical prediction $\exp(-Az)$ is accurate in almost all of the range, showing deviations from an exponential decay only at very small z values: These deviations are an expected effect because at small Δ_M we must have $P_M(\Delta_M, L) = P_M(0, L) - O(\Delta_M^2)$.

We computed the cumulant ratios

$$K = \langle \Delta^4 \rangle / \langle \Delta^2 \rangle^2, \qquad R = \langle \Delta^4 \rangle \langle \Delta^2 \rangle / \langle \Delta^3 \rangle^2 \qquad [11]$$

whose numerical values (depicted in Fig. 2, *Bottom*) compare well with the values predicted using Eq. **10**. These are only approximate predictions because both K and R depend on the behavior of $P_M(\Delta_M, L)$ in the region of small z where the large-deviation behavior $\exp(-Az)$ is not expected to hold. The ratio R was constructed in such a way to be less dependent on the value of the probability in the small z region: Its value is remarkably in better agreement with the theoretical predictions than the kurtosis K.

We also looked at the dependence of $A_{M,L}$ as a function of M/L. The theoretical predictions (derived in *Methods*) are shown in Fig. 3 and are in very good agreement with the numerical data.

Conclusions

The numerical evidence presented above strongly supports the correctness of the FPV prediction on the lower critical dimension $D_{lc} = 5/2$ and the scaling of the free energy interface barriers. It is remarkable that the corresponding exponents have a simple functional dependence on D and they do not show any of the usual anomalous corrections when extending below the upper critical dimension. This phenomenon is typical of interface energies in the broken-symmetry phase where these quantities are not changed by corrections to mean-field theory: It is also related to the decoupling of Goldstone-type modes at low momenta. Here the situation is far more complex because the analysis is based on nonlinear corrections and it does not match with perturbative corrections.

In spin glasses, one can define constrained connected correlation functions $C(x|Q) \equiv \langle q(x)q(0)\rangle_Q - Q^2$, where the average is done in a two-replica system where the total overlap is Q. Dimensional analysis implies that $C(x|Q) = B(Q)x^{-\alpha}$ with $\alpha = 4/5(D-5/2)$ in the region of $Q < Q_{EQ}$. In $D=3$ large lattices simulations give $\alpha(Q)$ independent from Q, equal to 0.38 ± 0.02 against the theoretical prediction of $2/5$ (33).

In momentum space the FPV prediction becomes $\tilde{C}(k|Q) \propto 1/(k^2)^{D/5+2}$. This last prediction on the momentum behavior poses more questions. An expansion around the mean field (34) in high dimensions gives two different exponents α, depending on the value of Q. At $Q=0$, $\alpha(0) = D-4$; at $0 < Q < Q_{EA}$, $\alpha(Q) = D-3$. These two predictions cross the FPV prediction at $D=10$ for $Q=0$ and at $D=5$ for $Q \neq 0$. It is unclear whether something special happens at these two dimensions.

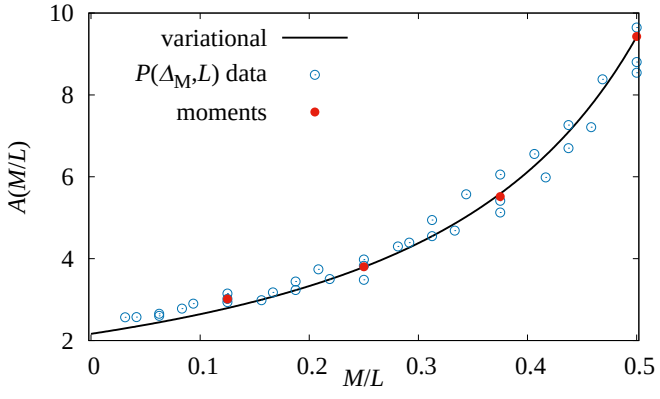

Fig. 3. The coefficient $A_{M,L}$ in the energy barrier (Eqs. **14** and **15**), obtained by (*i*) fitting Monte Carlo $P(\Delta_M; L)$ data (open circles) with $M = 1, \ldots, L/2$ and $L = 16, 24, 32$; (*ii*) fitting Eq. **15** to the second moment $\langle \Delta^2 \rangle$ (solid circles) at ratios $M/L = 1/8, 1/4, 3/8$ and $1/2$; and (*iii*) variational computation in the continuum limit (solid line) (*SI Appendix, The Computation of the Free Energy Barrier as a Function of M/L*). An overall factor to the variational data has been adjusted to match moments data (*Methods*).

Methods

Direct Measurement of the Interface Energy. We performed Monte Carlo simulations of the EA model with binary couplings, Eq. **2**, on the cubic lattice of size L with periodic boundary conditions for $L = 4, 6, 8, 10, 12, 14, 16, 20$ in $D=3$ and $L = 4, 5, 6, 7, 8, 9, 10, 12$ in $D=4$ by means of single-spin flip dynamics with the usual Metropolis algorithm and using parallel tempering (35–37) to improve decorrelation and convergence. The lowest temperatures simulated in the parallel-tempering protocol are $T = 0.7 \simeq 0.64 T_c$ for $D=3$ and $T = 1.4 \simeq 0.7 T_c$ for $D=4$ which are also the temperatures for which we show data in this work. We simulated $N_J = 12{,}800$ different instances of the system.

The simulation protocol we used to measure the interface barrier in the large Δ, $Q=0$ sector is the following:

i) We thermalize a given instance of the system S.
ii) Once equilibrium is reached, the system is replicated twice: The replica $S^{(+)}$ retains the periodic boundary condition; we label site coordinates as $i = i_1, \ldots, i_D$ in D dimensions; and we apply antiperiodic boundary conditions in the Dth direction to the replica $S^{(-)}$.
iii) We freeze spins on the $i_D = 0$ (hyper)plane on both $S^{(+)}$ and $S^{(-)}$ (we inhibit their update in the single-spin flip dynamics).
iv) We thermalize both $S^{(+)}$ and $S^{(-)}$ and compute $\Delta E = \langle E(S^{(-)}) - E(S^{(+)}) \rangle$, where $\langle \cdots \rangle$ is a thermal (Monte Carlo) average.
v) We repeat and collect statistics of ΔE over N_J samples.

If we compute overlaps between $S^{(+)}$ and $S^{(-)}$ on planes at fixed i_D

$$q(x) = \frac{1}{L^{D-1}} \sum_{i_1, \ldots, i_{D-1}} \sigma^{(-)}_{i_D = x} \sigma^{(+)}_{i_D = x}, \qquad [12]$$

in the limit of large L, $\Delta = |q(x=0) - q(x=L-1)|$ tends to the maximum allowed value, while $L^{-1}\sum_x q(x) \to 0$.

A related approach was followed before in ref. 38 to study the scaling properties of the interface energy in a different setting and with smaller system sizes, obtaining compatible results.

Large Deviations of the Overlap Fluctuations. To extract data for the distribution $P(\Delta_M, L)$ we took advantage of the Janus Collaboration's database (29–31). The dataset consists of many equilibrium configurations at different temperatures [in the number of O(100) independent spin configurations per sample and per temperature at the largest size] of 4,000 samples of size $L = 16$, 24 and 1,000 samples of size $L = 32$ of the $D=3$ EA model with binary couplings.

For each pair of spin configurations $\{\sigma\}$ and $\{\sigma'\}$ we compute the overlaps in boxes of size ML^2,

$$q_M(z) = \frac{1}{ML^2} \sum_{z \le i_D \le z+M-1} \sigma_i \sigma'_i, \qquad [13]$$

for $M = 1, \ldots, L/2$, and collect statistics for $\Delta_M = \frac{1}{2}|q_M(z) - q_M(z + L/2)|$ in the sector $Q_M = \frac{1}{2}|q_M(z) + q_M(z + L/2)| < 1/16$ (this is an arbitrary cutoff chosen to soften the $Q_M = 0$ constraint enough to have satisfactory statistics; other $1/2$ factors are chosen to normalize Q_M and Δ_M in $[0, 1]$). The FPV prediction for the distribution of Δ_M is

$$P(\Delta_M, L) \propto \exp\left[-A_{M,L} L^{1/2} \Delta_M^{5/2}\right], \qquad [14]$$

where the constant $A_{M,L}$ depends on the definition of the overlap, mainly on the boxes' geometry through the ratio M/L. The moments of the distribution in Eq. **14** are combinations of Euler's gamma functions

$$\langle \Delta_M^k \rangle = A_{M,L}^{2k/5} L^{-k/5} \frac{\Gamma\left((2k+2)/5\right)}{\Gamma\left(2/5\right)}, \qquad [15]$$

and cumulants such as those in Eq. **11** should not depend on either A or L. For large L the coefficients $A_{M,L}$ should not depend on L as long as M/L is kept fixed. We estimate values of A from our data in two ways: (*i*) by fitting Eq. **14** to $P(\Delta_M, L)$ data and (*ii*) by fitting Eq. **15** to L-dependent data at fixed M/L. Results are shown in Fig. 3. The extracted values compare well to estimates obtained in independent computations in the continuum limit (*SI Appendix, The Computation of the Free Energy Barrier as a Function of M/L*), which are represented in Fig. 3 as a solid line.

ACKNOWLEDGMENTS. We thank S. Franz who stimulated us in checking the FPV predictions on the scaling exponents, V. Astuti for very useful discussions on $\Delta F(L, \Delta)$, and the Janus Collaboration for letting us analyze Janus data. This project received funding from the European Research Council under the European Union's Horizon 2020 program (Grant 694925).

1. Wilson KG (1971) Renormalization group and critical phenomena. I. Renormalization group and the Kadanoff scaling picture. *Phys Rev B* 4:3174–3183.
2. Wilson KG (1971) Renormalization group and critical phenomena. II. Phase-space cell analysis of critical behavior. *Phys Rev B* 4:3184–3205.
3. Wilson KG, Fisher ME (1972) Critical exponents in 3.99 dimensions. *Phys Rev Lett* 28:240–243.
4. Polyakov AM (1975) Interaction of goldstone particles in two dimensions. Applications to ferromagnets and massive Yang-Mills fields. *Phys Lett B* 59: 79–81.
5. Migdal AA (1975) Phase transitions in gauge and spin-lattice systems. *Zh Eksp Teor Fiz* 69:1457.
6. Brezin E, Zinn-Justin J (1976) Spontaneous breakdown of continuous symmetries near two dimensions. *Phys Rev B* 14:3110.
7. Nelson DR, Pelcovits RA (1977) Momentum-shell recursion relations, anisotropic spins, and liquid crystals in $2 + \epsilon$ dimensions. *Phys Rev B* 16:2191.
8. Franz S, Parisi G, Virasoro M-A (1994) Interfaces and lower critical dimension in a spin glass model. *J Phys* 4:1657–1667.
9. Mermin ND, Wagner H (1966) Absence of ferromagnetism or antiferromagnetism in one- or two-dimensional isotropic Heisenberg models. *Phys Rev Lett* 17:1133–1136.
10. Hohenberg PC (1967) Existence of long-range order in one and two dimensions. *Phys Rev* 158:383–386.
11. Edwards SF, Anderson PW (1975) Theory of spin glasses. *J Phys F Metal Phys* 5:965–974.
12. Jing-Huei C, Lubensky T (1977) Mean field and $\epsilon-$expansion study of spin glasses. *Phys Rev B* 16:2106–2114.
13. Pytte E, Rudnick J (1979) Scaling, equation of state, and the instability of the spin-glass phase. *Phys Rev B* 19:3603–3621.
14. Harris A, Lubensky T, Jing-Huei C (1976) Critical properties of spin-glasses. *Phys Rev Lett* 36:415.
15. Green JE (1985) $\epsilon-$Expansion for the critical exponents of a vector spin glass. *J Phys A Math Gen* 18:L43–L47.
16. Gunnarsson K, et al. (1991) Static scaling in a short-range Ising spin glass. *Phys Rev B* 43:8199–8203.
17. Palassini M, Caracciolo S (1999) Universal finite-size scaling functions in the 3D Ising spin glass. *Phys Rev Lett* 82:5128–5131.
18. Ballesteros HG, et al. (2000) Critical behavior of the three-dimensional Ising spin glass. *Phys Rev B* 62:14237.
19. Boettcher S (2004) Stiffness exponents for lattice spin glasses in dimensions $d = 3, \ldots, 6$. *Euro Phys J B* 38:83–91.
20. Boettcher S (2004) Low-temperature excitations of dilute lattice spin glasses. *Europhys Lett* 67:453–459.
21. Boettcher S (2005) Stiffness of the Edwards-Anderson model in all dimensions. *Phys Rev Lett* 95:197205.
22. Fisher DS, Huse DA (1988) Equilibrium behavior of the spin-glass ordered phase. *Phys Rev B* 38:386–411.
23. Baity-Jesi M, et al. (2013) Critical parameters of the three-dimensional Ising spin glass. *Phys Rev B* 88:224416.
24. Baños RA, Fernandez LA, Martin-Mayor V, Young AP (2012) Correspondence between long-range and short-range spin glasses. *Phys Rev B* 86:134416.
25. Marinari E, Zuliani F (1999) Numerical simulations of the four-dimensional Edwards-Anderson spin glass with binary couplings *J Phys A Math Gen* 32:7447–7461.
26. Jörg T, Katzgraber HG (2008) Universality and universal finite-size scaling functions in four-dimensional Ising spin glasses. *Phys Rev B* 77:214426.
27. Hartmann AK (1999) Scaling of stiffness energy for three-dimensional $\pm$J Ising spin glasses. *Phys Rev E* 59:84–87.
28. Hartmann AK (1999) Calculation of ground states of four-dimensional $\pm$J Ising spin glasses. *Phys Rev E* 60:5135–5138.
29. Baños RA, et al. (2010) Nature of the spin-glass phase at experimental length scales. *J Stat Mech* 2010:P06026.
30. Baity-Jesi M, et al. (2014) Janus ii: A new generation application-driven computer for spin-system simulations. *Comput Phys Comm* 185:550–559.
31. Belletti F, et al. (2008) Simulating spin systems on IANUS, an FPGA-based computer. *Comput Phys Commun* 178:208–216.
32. Franz S, Jörg T, Parisi G (2009) Overlap interfaces in hierarchical spin-glass models. *J Stat Mech* 2009:P02002.
33. Belletti F, et al. (2009) An in-depth view of the microscopic dynamics of Ising spin glasses at fixed temperature. *J Stat Phys* 135:1121–1158.
34. De Dominicis C, Kondor I, Temesvari T (1998) Beyond the Sherrington-Kirkpatrick model. *Spin Glasses and Random Fields*, ed Young AP (World Scientific, Singapore) pp 119–160.
35. Geyer CJ (1991) Markov chain Monte Carlo maximum likelihood. Computing science and statistics. *Proceedings of the 23rd Symposium on the Interface*, pp 156–163.
36. Hukushima K, Nemoto K (1996) Exchange Monte Carlo method and application to spin glass simulations. *J Phys Soc Jpn* 65:1604.
37. Marinari E (1998) Optimized Monte Carlo methods. *Advances in Computer Simulation*, eds Kerstész J, Kondor I (Springer, Berlin), pp 50–81.
38. Contucci P, Giardinà C, Giberti C, Parisi G, Vernia C (2011) Interface energy in the Edwards-Anderson model. *J Stat Phys* 142:1–10.